

# Discretized Tikhonov regularization for Robin boundaries localization

Hui Cao<sup>a</sup>, Sergei V. Pereverzev<sup>b</sup>, Eva Sincich<sup>c</sup>

<sup>a</sup>*School of Mathematics and Computational Science, Sun Yat-sen University, Guangzhou, 510275, P.R. China*

<sup>b</sup>*Johann Radon Institute for Computational and Applied Mathematics, Austrian Academy of Sciences, Linz, A-4040, Austria*

<sup>c</sup>*Laboratory for Multiphase Processes, University of Nova Gorica, Slovenia*

---

## Abstract

We deal with a boundary detection problem arising in nondestructive testing of materials. The problem consists in recovering an unknown portion of the boundary, where a Robin condition is satisfied, with the use of a Cauchy data pair collected on the accessible part of the boundary. We combine a linearization argument with a Tikhonov regularization approach for the local reconstruction of the unknown defect. Moreover, we discuss the regularization parameter choice by means of the so called balancing principle and we present some numerical tests that show the efficiency of our method.

*Keywords:* Tikhonov regularization, Robin boundary condition, Free boundary problem, Balancing Principle, Local identification

---

## 1. Introduction

In this paper we deal with an inverse problem arising in corrosion detection. We consider a domain  $\Omega \subset \mathbb{R}^2$  which models a  $2D$  transverse section of a thin metallic specimen whose boundary is partly accessible and stays in contact with an aggressive environment. Hence, in order to detect the damage which is expected to occur in such a portion of the boundary, one has to rely on the electrostatic measurements of a potential  $u$  performed on the accessible portion.

---

*URL:* caohui6@mail.sysu.edu.cn (Hui Cao), sergei.pereverzyev@oeaw.ac.at (Sergei V. Pereverzev), eva.sincich@ung.si (Eva Sincich)

We are then lead to the study of the following elliptic boundary value problem

$$\begin{cases} \Delta u = 0, & \text{in } \Omega, \\ \frac{\partial u}{\partial \nu} = \Phi, & \text{on } \Gamma_A, \\ \frac{\partial u}{\partial \nu} + \gamma u = 0, & \text{on } \Gamma_I, \\ u = 0, & \text{on } \Gamma_D. \end{cases} \quad (1.1)$$

According to this model  $u$  is the harmonic potential in  $\Omega$ . We assume that the boundary of  $\Omega$  is decomposed in three open and disjoint subsets  $\Gamma_A, \Gamma_I, \Gamma_D$ . On the portion  $\Gamma_A$ , which is the one accessible to direct inspection, we prescribe a current density  $\Phi$  and we measure the corresponding voltage potential  $u|_{\Gamma_A}$ . The portion  $\Gamma_I$ , where the corrosion took place, is out of reach. On such a portion the potential  $u$  satisfies an homogeneous Robin condition, which models a resistive coupling with the exterior environment by means of the impedance coefficient  $\gamma$ .

In this paper we are interested in the numerical reconstruction issue of the unknown and damaged boundary  $\Gamma_I$  from the data collected on the accessible part of the boundary  $\Gamma_A$ , that is the Cauchy data pair  $(u|_{\Gamma_A}, \Phi)$ .

Boundary and parameter identification results related to this stationary inverse problem has been provided by many authors [1, 2, 3, 5, 9, 4, 10, 11, 12, 13, 14, 15, 16, 17].

Local uniqueness and conditional stability results for the inverse problem at hand are contained in [5] and constitute the theoretical setting on which our numerical analysis relies. The present local determination of corroded boundaries consists in the localization of a small perturbation  $\Gamma_{I,\theta}$  of a reference boundary  $\Gamma_I$ . It is convenient to introduce a small vector field  $\theta \in C_0^1(\Gamma_I)$  so that the damaged domain  $\Omega_\theta$  is such that

$$\partial\Omega_\theta = \overline{\Gamma_A} \cup \overline{\Gamma_D} \cup \overline{\Gamma_{I,\theta}}, \quad \Gamma_{I,\theta} = \{z \in \mathbb{R}^2 : z = w + \theta(w), w \in \Gamma_I\}.$$

Such a local approach combined with a linearization argument (see [5]) allows a reformulation of the problem of the localization of the unknown defect  $\Gamma_{I,\theta}$  as the identification of the unknown term  $\theta$  in a boundary condition of the type

$$\frac{\partial u'}{\partial \nu} + \gamma u' = \frac{d}{ds} \left( \theta \cdot \nu \frac{d}{ds} u \right) + \gamma \theta \cdot \nu (\gamma + 2H) u$$

at the portion  $\Gamma_I$ , where  $u'$  is a harmonic function satisfying homogeneous Neumann and Dirichlet conditions on  $\Gamma_A$  and  $\Gamma_D$  respectively,  $u$  is the solution of (1.1), and  $H$  denotes the curvature of the reference boundary  $\Gamma_I$ . As in [5] we carry over our analysis under the a-priori assumption of a constant  $\gamma$  such that  $2H(x) + \gamma > 0$  in  $\Gamma_I$  and we limit ourselves to the case of positive fluxes  $\Phi$  only.

We linearize the forward map  $F : \theta \mapsto u_\theta|_{\Gamma_A}$ , where  $u_\theta$  is the solution of the system (2.3) below, by its Fréchet derivative  $F'$  and take the *voltage contrast* on  $\Gamma_A$ , as the noisy right-hand term for the considered operator equation,

$$F'\theta = (u_\theta - u)|_{\Gamma_A}.$$

As in [13], we assume that the unavoidable measurement errors in *voltage contrast* are not smaller than the truncation error,  $o(\|\theta\|)$ . Therefore, if the noise level for voltage measurements is assumed to be  $\delta$ , then the noise level for the right-hand term of the above operator equation can be written as  $\tilde{\delta} = K\delta$ , where a constant  $K$  is not necessary to be precisely known. Our method is based on a discretized Tikhonov regularization argument where the regularization parameter is chosen by a balancing principle (cf. [6, 8, 20]). Such an *a posteriori* parameter choice can lead to a regularized solution with order-optimal accuracy. At the same time it can provide a reliable estimate for the constant  $K$ .

## 2. Local identification of the unknown boundary

In this section we shall collect the main identifiability results of which our reconstruction procedure and our numerical tests are a follow up. For a more detailed description we refer to [5].

We denote with  $\nu$  the outward normal to  $\Gamma_I$  and we assume that  $\theta$  is a vector field in  $C_0^1(\Gamma_I)$  having a nontrivial normal component  $\theta_\nu$  on  $\Gamma_I$ .

Let the Sobolev space  $H_0^1(\Omega, \Gamma_D)$  be defined as follows

$$H_0^1(\Omega, \Gamma_D) = \{v \in H^1(\Omega) : v = 0 \text{ on } \Gamma_D \text{ in the trace sense}\}. \quad (2.1)$$

We introduce the forward map  $F$

$$\begin{aligned} F : \quad C_0^1(\Gamma_I) &\rightarrow H^{\frac{1}{2}}(\Gamma_A) \\ \theta &\mapsto u_\theta|_{\Gamma_A} \end{aligned} \quad (2.2)$$

where  $u_\theta \in H_0^1(\Omega, \Gamma_D)$  is the solution to the elliptic problem

$$\begin{cases} \Delta u_\theta = 0 & \text{in } \Omega_\theta \\ \frac{\partial u_\theta}{\partial \nu} = \Phi & \text{on } \Gamma_A \\ \frac{\partial u_\theta}{\partial \nu} + \gamma u_\theta = 0 & \text{on } \Gamma_{I,\theta} \\ u = 0 & \text{on } \Gamma_D. \end{cases} \quad (2.3)$$

We recall the following differentiability property for the forward map  $F$ .

**Lemma 2.1.** *The operator  $F$  in (2.2) is Fréchet differentiable at zero. Indeed, consider the linear operator  $F' : C_0^1(\Gamma_I) \rightarrow H^{\frac{1}{2}}(\Gamma_A)$  defined as  $F'\theta = u'|_{\Gamma_A}$ , where  $u'$  is the solution to the boundary value problem*

$$\begin{cases} \Delta u' = 0 & \text{in } \Omega \\ \frac{\partial u'}{\partial \nu} = 0 & \text{on } \Gamma_A \\ \frac{\partial u'}{\partial \nu} + \gamma u' = \frac{d}{ds} \left( \theta_\nu \frac{d}{ds} u \right) + \gamma \theta_\nu (\gamma + 2H) u & \text{on } \Gamma_I \\ u' = 0 & \text{on } \Gamma_D, \end{cases} \quad (2.4)$$

the function  $u$  is the solution of (1.1) and  $H$  denotes the curvature of the boundary  $\Gamma_I$ . Then,

$$\frac{1}{\|\theta\|_{C_0^1(\Gamma_I)}} \|F(\theta) - F(0) - F'\theta\|_{H^{\frac{1}{2}}(\Gamma_A)} \rightarrow 0 \quad \text{as } \theta \rightarrow 0 \text{ in } C_0^1(\Gamma_I).$$

Let us also recall that a weak solution to (2.4) is a function  $u' \in H_0^1(\Omega, \Gamma_D)$  such that

$$\int_{\Omega} \nabla u' \nabla v + \int_{\Gamma_I} \gamma u' v = \int_{\Gamma_I} \gamma \theta_\nu (\gamma + H) u v - \int_{\Gamma_I} \theta_\nu \frac{d}{ds} u \frac{d}{ds} v \quad (2.5)$$

for all  $v \in H_0^1(\Omega, \Gamma_D)$ .

The following theorem ensures that the operator  $F'$  is injective, under some reasonable hypothesis. This property allows us to conclude that the solution  $\theta$  to our inverse problem is identifiable, at least for small perturbations. Moreover, we recall a conditional Lipschitz type upper bound for  $\theta$  on a suitable portion of  $\Gamma_I$  in terms of  $u'|_{\Gamma_A} = F'\theta$ , thus showing that the inversion of  $F'$  is not too much ill-behaved.

**Theorem 2.2.** *Let  $\Phi \in H^{\frac{1}{2}}(\Gamma_A)$  be nonnegative in the sense of distributions. Let us assume that  $2H(x) + \gamma > 0$  and  $\theta_\nu(x) \leq 0$  for any  $x \in \Gamma_I$ . Then  $F'$  is injective. Moreover, there exists a positive constant  $c > 0$  such that*

$$\|u'\|_{H^{\frac{1}{2}}(\Gamma_A)} \geq c \int_{\tilde{\Gamma}_I} |\theta|,$$

where  $\tilde{\Gamma}_I$  is an inner portion of the boundary  $\Gamma_I$ .

Finally, in the next theorem, we consider  $L^2(\Gamma_A)$  as codomain space of the operator  $F'$  introduced in Lemma 2.1 stating a compactness result.

**Theorem 2.3.** *The linear operator*

$$\begin{aligned} F' : \quad C_0^1(\Gamma_I) &\rightarrow L^2(\Gamma_A) \\ \theta &\mapsto u'|_{\Gamma_A} \end{aligned}$$

where  $u'$  is the solution to the boundary value problem (2.4), is compact.

### 3. Tikhonov regularization for a local reconstruction and an estimate of the accuracy

Here and in the following, with a slight abuse of notation, we shall denote by  $F'$  the compact operator

$$\begin{aligned} F' : \quad H_0^1(\Gamma_I) &\rightarrow L^2(\Gamma_A) \\ \theta &\mapsto u', \end{aligned} \tag{3.1}$$

where  $u'$  satisfies the weak formulation in (2.5) for any  $v \in H_0^1(\Omega, \Gamma_D)$ .

The existence and uniqueness of  $u' \in H_0^1(\Omega, \Gamma_D)$  follows from standard arguments on elliptic boundary value problems. Moreover, the compactness of  $F'$  in (3.1) follows along the lines of Theorem 4.5 in [5].

In view of this compactness property, the issue of the identification of  $\theta$  may be interpreted as the regularized inversion of the above compact operator  $F' = F'(\Gamma_I)$  between the Hilbert spaces  $H_0^1(\Gamma_I)$  and  $L^2(\Gamma_A)$ . Such kind of reformulation allows us to deal with the approximate inversion by the technique of Tikhonov regularization.

We are interested in finding the solution to operator equation

$$F'\theta = \bar{r} := u'|_{\Gamma_A}, \tag{3.2}$$

where instead of the exact data  $\bar{r}$ , a noisy version  $r^\delta$  is known. As in [13], if we linearize the forward map  $F$  defined in (2.2) by its Fréchet derivative, then by Lemma 2.1, we obtain

$$F'\theta = F(\theta) - F(0) + o(\|\theta\|),$$

i.e.

$$F'\theta = (u_\theta - u)|_{\Gamma_A} + o(\|\theta\|).$$

Here  $u_\theta|_{\Gamma_A}$  and  $u|_{\Gamma_A}$  are voltages measured in experiments. In practice they are usually given in a noisy form as  $u_\theta|_{\Gamma_A}^\delta$  and  $u|_{\Gamma_A}^\delta$  with  $\delta$  being the noise level for unavoidable experimental error for the measurements of the voltage. When  $\|\theta\|$  is rather small, one can assume that these measurement errors in *voltage contrast*  $(u_\theta - u)|_{\Gamma_A}$  have the same order of magnitude as the truncation error  $o(\|\theta\|)$ . Thus, we take

$$r^\delta := u_\theta^\delta|_{\Gamma_A} - u^\delta|_{\Gamma_A}$$

as the noisy right hand term for (3.2) and assume that

$$\|\bar{r} - r^\delta\|_{L^2(\Gamma_A)} \leq \tilde{\delta} = C\delta, \quad (3.3)$$

where a constant  $C$  is unknown.

If the Tikhonov regularization is applied to the ill-posed operator equation

$$F'\theta = r^\delta,$$

then the regularized solution solves

$$(F')^*F'\theta + \alpha I = (F')^*r^\delta \quad (3.4)$$

where  $\alpha > 0$  is the Tikhonov regularization parameter and  $I$  is the identity operator on space  $H_0^1(\Gamma_I)$ . It is well known that the solution to (3.4) will be the minimizer of the functional

$$\mathcal{J}(\theta) := \|F'\theta - r^\delta\|_{L^2(\Gamma_A)}^2 + \alpha\|\theta\|_{H_0^1(\Gamma_I)}^2. \quad (3.5)$$

Here, we assume the exact solution  $\theta$  belongs to the set of source condition

$$\mathcal{M}_h := \{s \in H_0^1(\Gamma_I) : s = h((F')^*F')w, \|w\| \leq 1\} \quad (3.6)$$

where  $h$  is an ‘index function’ defined on  $[0, \infty)$ , which is operator monotone (see [18, 19]) and satisfies the condition  $h(0) = 0$ . Moreover, it has been proven that

$$\sup_{0 < \lambda \leq b} \left| \frac{\alpha}{\alpha + \lambda} \right| h(\lambda) \leq h(\alpha) \quad \text{for all } \alpha \in (0, \bar{\alpha}] \quad (3.7)$$

and some  $\bar{\alpha} > 0$ .

Let us notice that  $\mathcal{J}(\theta)$  in (3.5) is the standard Tikhonov regularization functional, where the penalty term naturally is imposed in  $H_0^1$ -norm. Such a consideration can facilitate the analysis for the accuracy. Moreover, it is equivalent to the Tikhonov regularization functional considered in [13] with a penalty term based on the derivative of the regularized solution.

The discretization of the regularized problem (3.4) is realized by Galerkin method. The Galerkin approximation of Tikhonov-regularization consists in minimizing the above functional  $\mathcal{J}(\theta)$  in a finite-dimensional subspace  $X_n \subset H_0^1(\Gamma_I)$ . As usual, in Galerkin scheme, the discretized regularized solution  $\theta_{\alpha,n}^\delta$  is characterized by the variational equations

$$\langle F' \theta_{\alpha,n}^\delta - r^\delta, F' z \rangle + \alpha \langle \theta_{\alpha,n}^\delta, z \rangle = 0, \quad \forall z \in X_n, \quad (3.8)$$

or, equivalently,

$$\theta_{\alpha,n}^\delta = ((F'_n)^* F'_n + \alpha I)^{-1} (F'_n)^* r^\delta, \quad (3.9)$$

where  $F'_n := F' P_n$ , with  $P_n$  being the projection from  $H_0^1(\Gamma_I)$  onto  $X_n$ .

Let  $f_1, f_2, \dots, f_n$  be basis functions of  $X_n$ . If one decomposes  $\theta_{\alpha,n}^\delta$  into a linear combination of  $f_1, f_2, \dots, f_n$ , i.e.  $\theta_{\alpha,n}^\delta = \sum_{i=1}^n c_i f_i$ , then the coefficient vector  $\vec{c} = \{c_i\}_{i=1}^n$  can be obtained by solving a linear algebraic system,

$$(M + \alpha G) \vec{c} = R_\delta,$$

with the following matrices and vector,

$$\begin{aligned} M &:= \left( \langle F' f_i, F' f_j \rangle_{L^2(\Gamma_A)} \right)_{i,j=1}^n \\ G &:= \left( \langle f_i, f_j \rangle_{H_0^1(\Gamma_I)} \right)_{i,j=1}^n \\ R_\delta &:= \left\{ \langle F' f_i, r^\delta \rangle_{L^2(\Gamma_A)} \right\}_{i=1}^n. \end{aligned} \quad (3.10)$$

**Remark 3.1.** The adjoint operator  $(F')^*$  is not involved in the construction of  $\theta_{\alpha,n}^\delta$ . Theoretically,  $F' f_i$  can be obtained by solving the boundary value

system (2.4) and deriving the trace on  $\Gamma_A$ , where function  $\theta$  is replaced by  $f_i$ , for  $i = 1, \dots, n$ . Moreover, we do not need each  $F'f_i$  in an explicit form, but only its products in (3.10), which can be computed much more accurately than  $F'f_i$  itself.

According to the classical results on Tikhonov regularization for linear ill-posed problem and in view of (3.3) and (3.7), it holds that

$$\begin{aligned}
& \|\theta - \theta_{\alpha,n}^\delta\|_{H_0^1(\Gamma_I)} \\
& \leq \left\| \theta - ((F'_n)^* F'_n + \alpha I)^{-1} (F'_n)^* \bar{r} \right\|_{H_0^1(\Gamma_I)} \\
& \quad + \left\| ((F'_n)^* F'_n + \alpha I)^{-1} (F'_n)^* (\bar{r} - r^\delta) \right\|_{H_0^1(\Gamma_I)} \\
& \leq \left\| \theta - ((F'_n)^* F'_n + \alpha I)^{-1} (F'_n)^* \bar{r} \right\|_{H_0^1(\Gamma_I)} + \frac{C\delta}{2\sqrt{\alpha}}.
\end{aligned}$$

As in [19], we can estimate the noise free term as follows,

$$\begin{aligned}
& \left\| \theta - ((F'_n)^* F'_n + \alpha I)^{-1} (F'_n)^* \bar{r} \right\|_{H_0^1(\Gamma_I)} \\
& \leq \left\| \left( I - ((F'_n)^* F'_n + \alpha I)^{-1} (F'_n)^* F'_n \right) \theta \right\|_{H_0^1(\Gamma_I)} \\
& \quad + \left\| ((F'_n)^* F'_n + \alpha I)^{-1} (F'_n)^* F' (I - P_n) \theta \right\|_{H_0^1(\Gamma_I)} \\
& \leq \left\| \left( I - ((F'_n)^* F'_n + \alpha I)^{-1} (F'_n)^* F'_n \right) h((F'_n)^* F'_n) w \right\|_{H_0^1(\Gamma_I)} \\
& \quad + \left\| \left( I - ((F'_n)^* F'_n + \alpha I)^{-1} (F'_n)^* F'_n \right) (h((F')^* F') - h((F'_n)^* F'_n)) w \right\|_{H_0^1(\Gamma_I)} \\
& \quad + \frac{\|F' (I - P_n) \theta\|_{L^2(\Gamma_A)}}{\sqrt{\alpha}} \\
& \leq C_1 \left( h(\alpha) + h \left( \|F' (I - P_n)\|^2 \right) + \frac{\|F' (I - P_n)\|}{\sqrt{\alpha}} \right),
\end{aligned}$$

where the constant  $C_1$  does not depend on  $\alpha$  and  $n$ .

In view of the best possible order of accuracy without discretization being  $h(\alpha) + \delta/\sqrt{\alpha}$ , the discretization has to be chosen such that

$$\|F' (I - P_n) : H_0^1(\Gamma_I) \rightarrow L^2(\Gamma_A)\| \leq \delta. \quad (3.11)$$

Summing up the estimates above, we have the following theorem.



**Theorem 3.1.** *Under assumptions (3.3) and (3.6), and with discretization satisfying (3.11), there holds that*

$$\|\theta - \theta_{\alpha,n}^\delta\|_{H_0^1(\Gamma_I)} \leq \bar{K}h(\alpha) + K \frac{\delta}{\sqrt{\alpha}} \quad (3.12)$$

where the constants  $\bar{K}$  and  $K$  do not depend on  $\alpha$  and  $\delta$ .

#### 4. Parameter choice rule based on the balancing principle

In this section, we give a regularization parameter choice rule based on the balancing principle developed in [6, 7, 20]. The essential idea of this principle is to choose the regularization parameter  $\alpha$  balancing the two parts in error estimate (3.12). As a posteriori parameter choice rule, the balancing principle can select regularization parameter in an adaptive way without a priori knowledge of the solution set (3.6). That is, the index function  $h$  in the bound (3.12), which indicates the smoothness of  $\theta$  as shown in (3.6), does not need to be known. At the same time, it does not require to know the precise noise level, either. In our model problem, constant  $C$  in (3.3) indicating the precise noise level is unknown, which leads to  $K$  in (3.12) is also unknown. A reference noise level  $\delta$  is sufficient for the performance of the balancing principle. The regularization parameter chosen by the balancing principle leads to a regularized solution with an order-optimal accuracy.

Assume that the projection  $P_n$  is chosen with  $n = n(F', \delta)$  such that (3.11) is satisfied. Let  $\theta_\alpha^\delta := \theta_{\alpha, n(F', \delta)}^\delta$ .

We select parameter  $\alpha$  from the geometric sequence

$$\Delta := \{\alpha_n = \alpha_0 q^n, \quad n = 0, 1, \dots, N\},$$

with  $q > 1$ , sufficiently small  $\alpha_0$ , and sufficiently large  $N$  such that  $\alpha_{N-1} \leq 1 < \alpha_N$ .

For any given  $K$ , one can choose the parameter from  $\Delta(\alpha_0, q, N)$  by the following adaptive strategy,

$$\alpha(K) = \max \left\{ \alpha_n \in \Delta : \|\theta_{\alpha_n}^\delta - \theta_{\alpha_m}^\delta\|_{H_0^1(\Gamma_I)} \leq K\delta \left( \frac{3}{\sqrt{\alpha_n}} + \frac{1}{\sqrt{\alpha_m}} \right), \quad m = 0, 1, \dots, n-1 \right\}. \quad (4.1)$$

We further rely on the assumption that a two-sided estimate

$$cK \frac{\delta}{\sqrt{\alpha}} \leq \|\theta_\alpha^0 - \theta_\alpha^\delta\|_{H_0^1(\Gamma_I)} \leq K \frac{\delta}{\sqrt{\alpha}}. \quad (4.2)$$

holds for some  $c \in (0, 1)$ , where  $\theta_\alpha^0$  is defined by (3.9) with  $r^\delta$  being taken as  $\bar{r}$ . The upper estimate in (4.2) is due to (3.12). As to the lower estimate, it just suggests that the noise propagation error is not that small. If the lower estimate is not satisfied, it just means that our estimate to noise level is too pessimistic. However this will not cause a problem, since later we shall show that under assumption (4.2) balancing principle can provide an order-optimal accuracy.

Now, consider the following hypothesis set of possible values of the constant  $K$

$$\mathcal{K} = \{k_j = k_0 p^j, \quad j = 0, 1, \dots, M\}, \quad p > 1,$$

and assume that there are two adjacent terms  $k_l, k_{l+1} \in \mathcal{K}$  such that

$$k_l \leq cK \leq K \leq k_{l+1}. \quad (4.3)$$

In fact, each element in  $\mathcal{K}$  can be viewed as a candidate for the estimator to constant  $K$ . Our aim is to detect  $k_{l+1}$  (or say  $k_l$ ) among the elements in  $\mathcal{K}$ , and to use  $k_{l+1}$  in adaptive strategy (4.1) to obtain a parameter  $\alpha$ .

In view of (4.2) and (4.3), if the hypothesis  $k_j \in \mathcal{K}$  for  $K$  is chosen too small, i.e.,  $k_j \leq k_l$  then, as it is shown in [6, 20], the corresponding regularization parameter  $\alpha(k_j)$  will be smaller than a threshold depending on  $\alpha_0$  and  $p$ . Thus, if

$$\alpha(k_i) := \min \left\{ \alpha(k_j) \geq 9\alpha_0 \left( \frac{p^2 + 1}{p - 1} \right)^2 \right\}, \quad (4.4)$$

then there holds that, either  $i = l$ , or  $i = l + 1$ .

In order to guarantee the regularized solution is stable enough, we choose final regularization parameter as

$$\alpha_+ = \alpha(k_{i+1}).$$

With such a choice  $\alpha_+$ , we have the following theorem.

**Theorem 4.1.** *Under the assumptions above, there holds*

$$\|\theta - \theta_{\alpha_+}^\delta\|_{H_0^1(\Gamma_I)} \leq 6p^2 \sqrt{q} \bar{K} h(\tilde{h}^{-1}(K\delta)),$$

where  $\tilde{h}(t) = \bar{K}h(t)\sqrt{t}$ ,  $\bar{K}$  is the constant from estimation (3.12), and  $\tilde{h}^{-1}$  is the inverse function of  $\tilde{h}$ .

Note that from [18] it follows that the error bound indicated in Theorem 4.1 is order-optimal, i.e., it is only worse by a constant factor  $3p^2\sqrt{q}$  than *a priori* optimal bound  $2\bar{K}h(\tilde{h}^{-1}(K\delta))$ . If index function  $h$  in the source condition (3.6) is given as  $h(\lambda) = c\lambda^\nu$ ,  $0 < \nu \leq 1$ , then  $h(\tilde{h}^{-1}(K\delta)) = O(\delta^{\frac{2\nu}{2\nu+1}})$ , which coincides with the classical rate for Tikhonov regularization.

**Remark 4.1.** *The proof of Theorem 4.1 can be referred to [6] or [7]. For the general discussions on the application of the balancing principle with two flexible parameters, one can refer to [20].*

## 5. Numerical tests

In this section, we present some numerical examples to illustrate the theoretical results obtained above.

In Examples 1-3, we consider the corrosion problem in (1.1) with

$$\begin{aligned}\Omega &= (0, \pi) \times (0, 1), \\ \Gamma_A &= (0, \pi) \times \{0\}, \\ \Gamma_I &= (0, \pi) \times \{1\}, \\ \Gamma_D &= \{0\} \times (0, 1) \cup \{\pi\} \times (0, 1).\end{aligned}$$

On such a rectangle domain, if the flux  $\Phi = \sin(x)$  is given on  $\Gamma_A$ , then the solution to (1.1) is in the form of

$$u(x, y) = \left( -\sinh(y) + \frac{\gamma \sinh(1) + \cosh(1)}{\sinh(1) + \gamma \cosh(1)} \cosh y \right) \sin(x).$$

with  $\gamma > 0$ . We test the same flux  $\Phi = \sin(x)$  in Examples 1-3.

### Example 1.

In this example the vector field  $\theta$  is given as  $\theta = (0, \theta_2(x))$  with

$$\theta_2(x) = \int_0^x \theta_2'(t) dt, \quad \text{where } \theta_2(0) = 0,$$

and

$$\theta_2'(x) = \begin{cases} \frac{-\cot(x) + \gamma \sqrt{\cot^2(x) - \gamma^2 + 1}}{\cot^2(x) - \gamma}, & 0 \leq x < \frac{\pi}{2}, \\ \frac{-\cot(x) - \gamma \sqrt{\cot^2(x) - \gamma^2 + 1}}{\cot^2(x) - \gamma}, & \frac{\pi}{2} \leq x \leq \pi, \end{cases}$$

with the constant  $\gamma$  such that  $0 < \gamma < 1$ . Such a choice of  $\theta$  corresponds to

$$u_\theta(x, y) = \exp(-y) \sin(x)$$

solving (2.3).

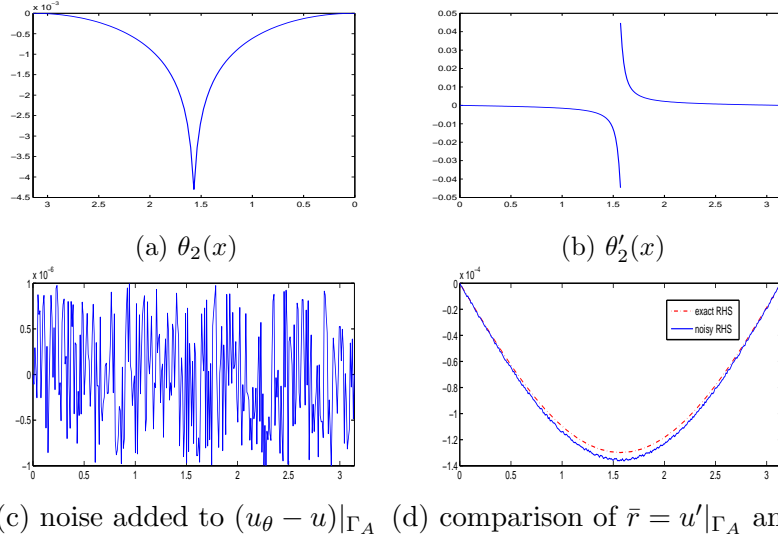


Figure 1: Functions in Example 1 with  $\gamma = 0.999$ .

As we mentioned in the Introduction, the impedance coefficient  $\gamma$  depending on the exterior environment should be a fixed constant in the model problem (1.1). However, in this particular example, the scale of  $\theta$  depends on  $\gamma$ . On the other hand, our linearization approach by truncation can only work when  $\|\theta\|$  is rather small. Thus, in this example we test different values of  $\gamma$  which are all quite close to 1. Figures 1 (a) and (b) illustrate the behaviors of  $\theta_2(x)$  and  $\theta'_2(x)$  when  $\gamma = 0.999$ . In order to simulate the error arising in experiment measurements, we add random noise to each grid involved in calculation, i.e. we take

$$r^\delta = (u_\theta - u)|_{\Gamma_A} + \xi\delta,$$

where  $\xi$  is random variable with range  $[-1, 1]$  and the reference noise level  $\delta = 10^{-6}$ . Figure 1 (c) and (d) show the additional noise  $\xi\delta$  and the comparison of  $\bar{r} = u'|_{\Gamma_A}$  and  $r^\delta$  in the case  $\gamma = 0.999$ .

In all of the following tests, the discretization level in (3.8) is taken as  $n = 20$  and the regularization parameter  $\alpha$  is chosen by the balancing principle

described in Section 4. In the case of  $\gamma = 0.999$ , the parameters in the implementation of the balancing principle are settled as follows:

$$\begin{aligned}\Delta &= \{\alpha_n = \alpha_0 q^n, \quad n = 0, 1, \dots, N\}, \quad \alpha_0 = 1 \cdot 10^{-11}, \quad q = 1.3, \quad N = 69; \\ \mathcal{K} &= \{k_j = k_0 p^j, \quad j = 0, 1, \dots, M\}, \quad k_0 = 0.006, \quad p = 1.3, \quad M = 19.\end{aligned}$$

Sequence  $\{\alpha(k_j)\}_{j=0}^{19}$  produced by (4.1) with  $K$  replaced by  $k_j$  results in

$$\begin{aligned}4.827 \cdot 10^{-11}, & \quad 8.157 \cdot 10^{-11}, \quad 1.379 \cdot 10^{-10}, \quad 3.937 \cdot 10^{-10}, \quad 1.900 \cdot 10^{-9}, \\ 9.173 \cdot 10^{-9}, & \quad 3.406 \cdot 10^{-8}, \quad 7.482 \cdot 10^{-8}, \quad 9.728 \cdot 10^{-8}, \quad 1.265 \cdot 10^{-7}, \\ 1.644 \cdot 10^{-7}, & \quad 2.778 \cdot 10^{-7}, \quad 3.612 \cdot 10^{-7}, \quad 6.104 \cdot 10^{-7}, \quad 1.341 \cdot 10^{-6}, \\ 2.946 \cdot 10^{-6}, & \quad 8.415 \cdot 10^{-6}, \quad 1.094 \cdot 10^{-5}, \quad 1.422 \cdot 10^{-5}, \quad 1.849 \cdot 10^{-5}.\end{aligned}$$

For the parameters designed as above, the value of the threshold is calculated as  $9\alpha_0 \left(\frac{p^2+1}{p-1}\right)^2 = 7.236 \cdot 10^{-9}$ . Then  $\alpha_+ = \alpha(k_7) = 3.406 \cdot 10^{-8}$ . At the same time, we obtain an estimate to  $K$  as  $k_7 = 0.0290$ , which suggests the true noise level  $K\delta$  is about  $2.90 \cdot 10^{-8}$ .

Table 1 summarizes the results for the other values of  $\gamma$  in Example 1. Here we take different reference noise level  $\delta$  according to  $\gamma$ , because, as we mentioned, in this particular example,  $\gamma$  determines the scale of  $\theta$  and furthermore the truncation error. In Table 1,  $Err_{h1} := \|\theta - \theta_{\alpha_+}^\delta\|_{H^1(\Gamma_I)}$  and  $Err_{l2} := \|\theta - \theta_{\alpha_+}^\delta\|_{L^2(\Gamma_I)}$  denote the errors in the corresponding norms. The reconstructed functions  $\theta_{\alpha_+}^\delta$  are displayed in Figure 2.

## Example 2.

In this example, the vector field  $\theta = (0, \theta_2(x))$  to be identified is similar to what is considered in [13], where  $\theta_2(x)$  is a piecewise linear function, as shown in Figure 3. In contrast to Example 1, we do not assume that  $\gamma \in (0, 1)$ , and test two cases:  $\gamma = 1$ ,  $\gamma = 10$ . The solution of (2.3) and

| $\gamma$ | $\delta$  | $K$    | $\alpha_+$            | $Err_{h1}$ | $Err_{l2}$            |
|----------|-----------|--------|-----------------------|------------|-----------------------|
| 0.9999   | $10^{-8}$ | 0.0489 | $2.015 \cdot 10^{-8}$ | 0.0012     | $9.134 \cdot 10^{-5}$ |
| 0.999    | $10^{-6}$ | 0.0290 | $3.406 \cdot 10^{-8}$ | 0.0080     | $6.127 \cdot 10^{-4}$ |
| 0.99     | $10^{-5}$ | 0.0636 | $1.265 \cdot 10^{-7}$ | 0.0438     | 0.0038                |
| 0.95     | $10^{-4}$ | 0.0489 | $5.756 \cdot 10^{-8}$ | 0.1482     | 0.0308                |

Table 1: Test results for Example 1.

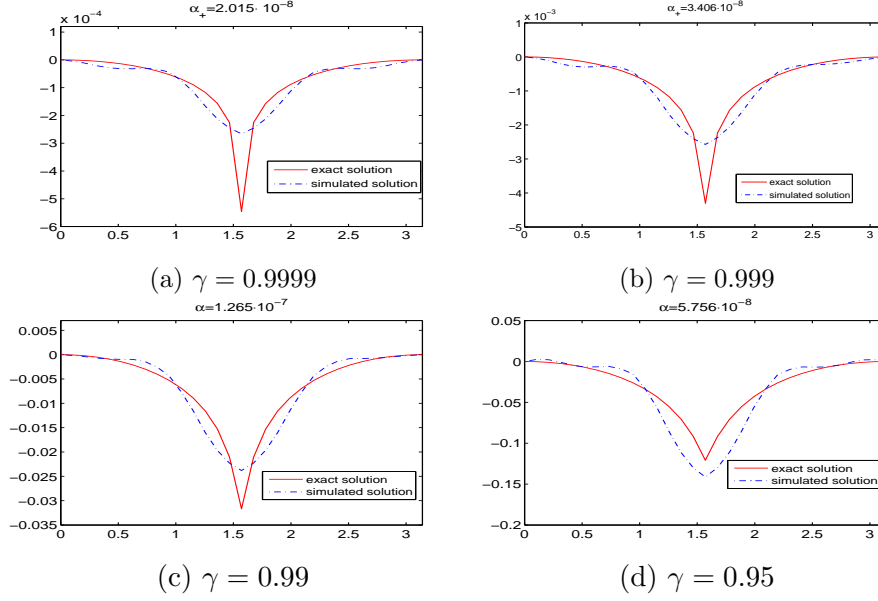


Figure 2: The simulated solutions  $\theta_{\alpha_+}^\delta$  in Example 1.

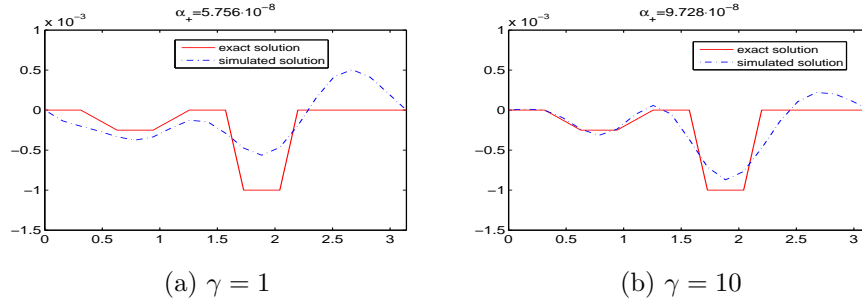


Figure 3: The simulated solutions  $\theta_{\alpha_+}^\delta$  in Example 2.

| $\gamma$ | $\delta$  | $K$    | $\alpha_+$            | $Err_{h1}$ | $Err_{l2}$            |
|----------|-----------|--------|-----------------------|------------|-----------------------|
| 1        | $10^{-7}$ | 0.3937 | $5.756 \cdot 10^{-8}$ | 0.0031     | $3.565 \cdot 10^{-4}$ |
| 10       | $10^{-7}$ | 0.5119 | $9.728 \cdot 10^{-8}$ | 0.0030     | $2.622 \cdot 10^{-4}$ |

Table 2: Test results for Example 2.

its trace  $u_\theta|_{\Gamma_A}$  are generated numerically. We simulate point-wise random noise in each discretization note on  $\Gamma_A$  with reference level  $\delta = 10^{-7}$ , and  $\alpha_+$  is chosen according to the balancing principle under such a value of  $\delta$ .

The approximations  $\theta_{\alpha+}^\delta$  are displayed in Figure 3 and the test results are summarized in Table 2.

**Example 3.**

In this example, we take the vector field  $\theta = (0, \theta_2(x))$  with

$$\theta_2(x) = h - \sqrt{\left(\frac{\pi}{2}\right)^2 + h^2 - \left(x - \frac{\pi}{2}\right)^2}, \quad 0 < x < \pi,$$

as shown in Figure 4. Here one can change the value of the constant  $h > 0$  to

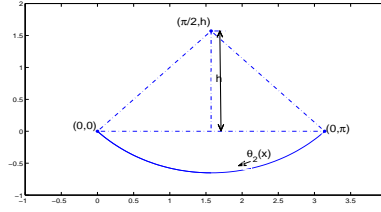


Figure 4: An illustration for  $\theta_2(x)$  in Example 3.

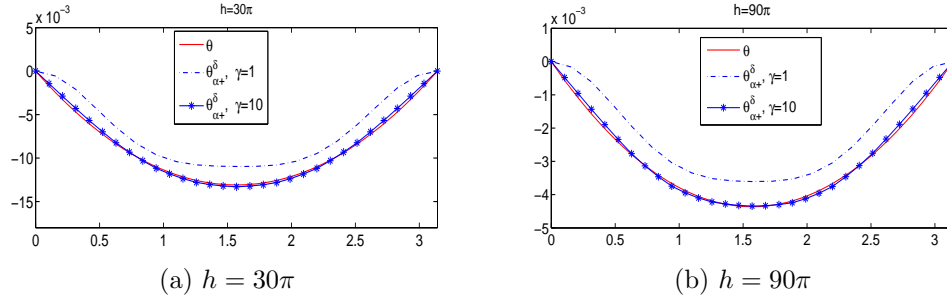


Figure 5: The simulated solutions  $\theta_{\alpha+}^\delta$  in Example 3.

adjust the scale of  $\theta$ . The solution  $u_\theta$  and its trace on  $\Gamma_A$  in this example are also obtained numerically. In order to guarantee that the scale of  $\theta$  is small enough such that the truncation method can work well, we test  $h = 30\pi$  and  $h = 90\pi$ . In both cases, larger value of  $\gamma$  may make the problem less ill-posed and result in better reconstruction. The approximations  $\theta_{\alpha+}^\delta$  are displayed in Figure 5 and the test results are summarized in Table 3.

| h       | $\gamma$ | $\delta$  | $K$    | $\alpha_+$            | $Err_{h1}$            | $Err_{l2}$            |
|---------|----------|-----------|--------|-----------------------|-----------------------|-----------------------|
| $30\pi$ | 1        | $10^{-5}$ | 0.0371 | $1.341 \cdot 10^{-6}$ | 0.0079                | 0.0034                |
|         | 10       | $10^{-5}$ | 0.0371 | $1.849 \cdot 10^{-5}$ | 0.0016                | $4.273 \cdot 10^{-4}$ |
| $90\pi$ | 1        | $10^{-7}$ | 0.1379 | $3.611 \cdot 10^{-6}$ | 0.0027                | 0.0013                |
|         | 10       | $10^{-7}$ | 0.1060 | $1.743 \cdot 10^{-6}$ | $6.300 \cdot 10^{-4}$ | $1.340 \cdot 10^{-4}$ |

Table 3: Test results for Example 3.

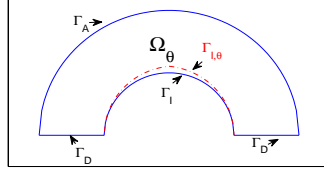


Figure 6: Domain  $\Omega_\theta$  in Example 4.

#### Example 4.

In the last example, we consider a domain  $\Omega$  given as a half annulus bounded by the following curves (see Figure 6).

$$\begin{aligned}\Gamma_A &= \left\{ (x, y) : y = \sqrt{4 - x^2}, -2 < x < 2 \right\}, \\ \Gamma_I &= \left\{ (x, y) : y = \sqrt{1 - x^2}, -1 < x < 1 \right\}, \\ \Gamma_D &= \left\{ (x, y) : y = 0, 1 < |x| < 2 \right\}.\end{aligned}$$

For flux  $\Phi = y$  on  $\Gamma_A$ , the function  $u$  solving (1.1) can be written as

| $\gamma$ | $\delta$  | $K$    | $\alpha_+$            | $Err_{h1}$ | $Err_{l2}$ |
|----------|-----------|--------|-----------------------|------------|------------|
| 0.99     | $10^{-5}$ | 0.0816 | $1.032 \cdot 10^{-5}$ | 0.0057     | 0.0028     |
| 0.9      | $10^{-4}$ | 0.0816 | $1.032 \cdot 10^{-5}$ | 0.0708     | 0.0384     |

Table 4: Test results for Example 4.

$$u(x, y) = Ay + \frac{By}{x^2 + y^2}, \text{ where } A = 1 + \frac{B}{4} \text{ and } B = \frac{1 - \gamma}{\frac{5}{4}\gamma + \frac{3}{4}},$$



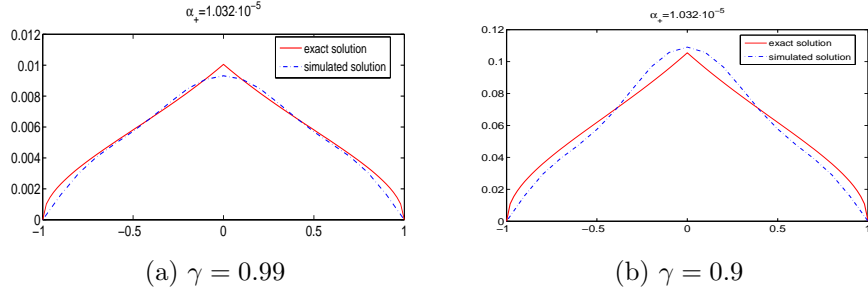


Figure 7: The simulated solutions  $\theta_{\alpha_+}^\delta$  in Example 4.

with  $0 < \gamma < 1$ . For vector field  $\theta = (0, \theta_2(x))$ , we consider  $\theta_2(x) = \varphi(x) - \sqrt{1 - x^2}$ , where

$$\varphi(x) = \begin{cases} \frac{1}{\gamma} \sqrt{1 - (\gamma x + \gamma - 1)^2}, & -1 < x \leq 0, \\ \frac{1}{\gamma} \sqrt{1 - (\gamma x - \gamma + 1)^2}, & 0 \leq x \leq 1. \end{cases}$$

It can be verified that  $u_\theta(x, y) = y$  solves (2.3) in  $\Omega_\theta$ .

In this example  $\gamma$  also determines the scale of  $\theta$ . Thus, we take the values of  $\gamma$  very close to 1. The approximations  $\theta_{\alpha_+}^\delta$  are displayed in Figure 7 and the test results are summarized in Table 4.

We would like to note that in all considered examples the balancing principle (4.1), (4.4) has been implemented with the same values of the design parameters  $\alpha_0$ ,  $p$  and  $q$ , because the domain  $\Omega$  and the operator  $F'$  are the same for all examples. This suggests that in practice, for a given domain  $\Omega$  the parameters  $\alpha_0$ ,  $p$  and  $q$  can be determined in the experiments with a problem (2.4) where a solution is known, and then kept for studying all other problems (2.3) in the given domain  $\Omega$ .

Both the theoretical and numerical results suggest that the linearization approach considered in this paper can perform well for the identification of the corroded boundary only on condition that the scale of this boundary function is quite small. This is the limitation of the approach. However, in practice one certainly does not expect too much corrosion taking place to the metallic specimen.

## Acknowledgement

This research was partially supported by Natural Science Foundation of China (No.11201497), Foundation for Distinguished Young Talents in Higher Education of Guangdong, China (No. LYM11007), Guangdong Provincial Government of China through the “Computational Science Innovative Research Team” program, Guangdong Province Key Laboratory of Computational Science at the Sun Yat-sen University and the PRIN 20089PWTPS project funded by the Italian Ministry for Education, University and Research (MIUR). S.V.P. is partially supported by the grant P25424 of the Austrian Science Fund (FWF). E.S. wishes to thank the Department of Mathematics and Geosciences of the University of Trieste (Italy) for partly supporting her work by a research grant. Part of this work was done while E.S. was visiting the Sun Yat-sen University. She also wishes to express her gratitude to the School of Mathematics and Computational Science for the kind hospitality.

## References

- [1] G. Alessandrini, L. Del Piero, L. Rondi, Stable determination of corrosion by a single electrostatic measurement, *Inverse Problems* 19 (2003), 973-984.
- [2] G. Alessandrini, E. Sincich, Detecting nonlinear corrosion by electrostatic measurements, *Applicable Analysis* 85 (2006), 107-128.
- [3] G. Alessandrini, E. Sincich, Solving elliptic Cauchy problems and the identification of nonlinear corrosion, *J. Comput. Appl. Math.* 198 (2007), 307-320.
- [4] V. Bacchelli, Uniqueness for the determination of unknown boundary and impedance with homogeneous Robin condition, *Inverse Problems* 25 (2009), 015004 (4pp).
- [5] E. Cabib, D. Fasino, E. Sincich, Linearization of a free boundary problem in corrosion detection, *J. Math. Anal. Appl.* 378 (2011), 700-709.
- [6] H. Cao, S. Pereverzev, Natural linearization for the identification of a diffusion coefficient in a quasi-linear parabolic system from short-time observations, *Inverse Problems* 22 (2006), 2311-2330.

- [7] H. Cao, M. V. Klibanov, S. V. Pereverzev, A Carleman estimate and the balancing principle in the quasi-reversibility method for solving Cauchy problem for the Laplace equation, *Inverse Problems* 25 (2009), 035005, 21 pp.
- [8] H. Cao, S. V. Pereverzev, Balancing principle for the regularization of elliptic Cauchy problems, *Inverse Problems* 23 (2007), 1943-1961.
- [9] H. Cao, S. V. Pereverzev, E. Sincich, Natural linearization for corrosion identification, *Journal of Physics: Conference Series* 135 (2008) 012027.
- [10] F. Cakoni, R. Kress, Integral equations for inverse problems in corrosion detection from partial Cauchy data, *Inverse Problems and Imaging* 1 (2007), 229-245.
- [11] S. Chaabane, S. Jaoua, Identification of Robin coefficients by means of boundary measurements, *Inverse Problems* 15 (1999), 1425-1438.
- [12] D. Fasino, G. Inglese, Recovering unknown terms in a nonlinear boundary condition for the Laplace's equation, *IMA J. Appl. Math.* 71 (2006), 832-852.
- [13] D. Fasino, G. Inglese, F. Mariani, Corrosion detection in conducting boundaries: II. Linearization, stability and discretization, *Inverse Problems* 23 (2007), 1101-1114.
- [14] P. G. Kaup, F. Santosa, Nondestructing evaluation of corrosion damage using electrostatic measurements, *J. Nondestructive Eval.* 14 (1995), 127-136.
- [15] P. Kügler, E. Sincich, Logarithmic convergence rates for the identification of a nonlinear Robin coefficient, *J. Math. Anal. Appl.* 259 (2009), 451-463.
- [16] E. Sincich, Lipschitz stability for the inverse Robin problem, *Inverse Problems* 23 (2007), 1311-1326.
- [17] E. Sincich, Stability for the determination of unknown boundary and impedance with a Robin boundary condition, *SIAM J. Math. Anal.* 42 (2010), 2922-2943.

- [18] P. Mathé, S. V. Pereverzev, Geometry of linear ill-posed problems in variable Hilbert scales. *Inverse Problems* 19 (2003), 789–803.
- [19] P. Mathé, S. V. Pereverzev, Discretization strategy for linear ill-posed problems in variable Hilbert scales. *Inverse Problems* 19 (2003), 1263–1277.
- [20] R. D. Lazarov, S. Lu, S. V. Pereverzev, On the balancing principle for some problems of numerical analysis, *Numer. Math.* 106 (2007), 659–689.